

CATEGORIZING LINEAR THEORIES FOR ATOMIZING ROUND JETS

Sam S. Yoon and Stephen D. Heister

School of Aeronautics and Astronautics, Purdue University, West Lafayette, Indiana, USA

This article compares and contrasts linear stability analyses based on the deformations of an infinite liquid column and due to boundary-layer vorticity imparted to the free surface from the orifice exit plane. The bulk of the prior works, which date back to Kelvin-Helmholtz [1], Rayleigh [2], Weber [3], Taylor [4], Ponstein [5], Levich [6], Sterling and Sleicher [7], and Reitz and Bracco [8], have focused on the liquid column analysis. Though used to a lesser extent, the boundary-layer instability analysis by Brennen [9] can also be used to predict the dominant wavelength of the laminar jet. Differences between the two approaches are highlighted for simple injection conditions and injector geometries.

1. INTRODUCTION

The linear theory associated with primary atomization of a liquid jet is well established and much studied. More recently, nonlinear analyses have served to compliment the linear results and explain the presence of satellite droplets which have frequently been observed in low-speed jets. At higher jet speeds, it becomes more difficult to assess the value of linear theories because turbulence and secondary atomization become important contributors and because the jet surface is often obscured by droplets. In spite of these drawbacks, many of today's atomization models draw heavily from the linear theories based on a column of liquid exposed to a high-velocity gas shear flow.

The biggest drawback of these theories is that there is no mechanism to include effects of the orifice geometry on the possible wavelengths introduced to the liquid surface. A notable exception here is the work of Hoyt and Taylor [10–12], which focused on the boundary-layer behavior at the orifice exit plane as a significant player in the subsequent instabilities observed in the jet. Drawing from a boundary-layer-based instability analysis due to Brennen [9], these researchers showed that the wavelengths observed in their carefully controlled experiment were in agreement with those predicted using Brennen's theory.

The aim of this short article is to compare and contrast these approaches and to assess potentially important contributions of other researchers which have not been frequently cited in prior literature. In this context, we provide a brief review of linear stability results and highlight similarities and differences in the various approaches. Specific examples are considered to illustrate differences between liquid column-based and boundary-layer-based approaches.

The authors gratefully acknowledge the support of the Air Force Office of Scientific Research (AFOSR) and Dr. Mitat Birkan under grant number F49620-99-1-0092.

2. LORD RAYLEIGH'S ANALYSIS

Probably the most famous and pioneering stability analysis for the liquid jet was developed by Lord Rayleigh [2]. Rayleigh considered the infinitely long, inviscid column of liquid with negligible influence from the gas phase. He hypothesized that an infinitesimal disturbance will cause the jet to break up under a capillary-based instability. The famous dispersion relation he obtained is as follows:

$$\omega^2 = \frac{\sigma}{\rho_l a^3} (1 - k^2 a^3) k a \frac{I_1(ka)}{I_0(ka)} \quad (1)$$

where $\omega = \omega_r + i\omega_i$ (i.e., ω_r = growth rate, $i = \sqrt{-1}$, and ω_i = frequency of oscillation), σ = surface tension of the liquid, ρ_l = liquid density, a = orifice radius, k = wavenumber = $2\pi/\lambda$ (i.e., λ = wavelength), and $I_1(ka)$ and $I_0(ka)$ are modified Bessel functions of the first kind. By expanding the Bessel functions in a power series and computing the maximum of the ω versus ka curve, he obtained the result:

$$\omega_m = 0.97 \sqrt{\frac{\sigma}{\rho_l a^3}} \quad (2)$$

for which the corresponding wavenumber and wavelength are

$$ka = 0.696 \approx 0.7 \quad \lambda = 4.51d \quad (3)$$

There are numerous experimental confirmations of Rayleigh's wavelength appearing in low-speed jets. Many researchers have extended the result to the fully nonlinear regime and assumed that the jet will actually fragment into sections $4.51d$ in length, which leads to a predicted droplet diameter of about $1.89d$ as shown in Fig. 1. While such conditions can be generated with a carefully controlled perturbation in an experiment, more commonly the jet is shown to bifurcate into two drops per wavelength; the presence of the satellite drops are not predicted from linear theory, but numerous nonlinear results [13–17] have confirmed their presence and agree well with size measurements from a variety of experiments.

The Rayleigh jet is of course the simplest of all cases in that aerodynamic interactions with the gas are neglected. The low jet velocities associated with this flow regime also imply that instabilities emanating from the boundary layer inside the orifice are necessarily small. For these reasons, there is good agreement between experiment and theory for a variety of orifice designs.

3. WEBER'S EQUATION

Weber [3] extended Rayleigh's analysis by adding the effect of viscosity of the jet, which gives:

$$\omega^2 + \frac{3\mu}{\rho_l a^2} (ka)^2 \omega = \frac{\sigma}{2\rho_l a^3} (1 - k^2 a^2) k^2 a^2 \quad (4)$$

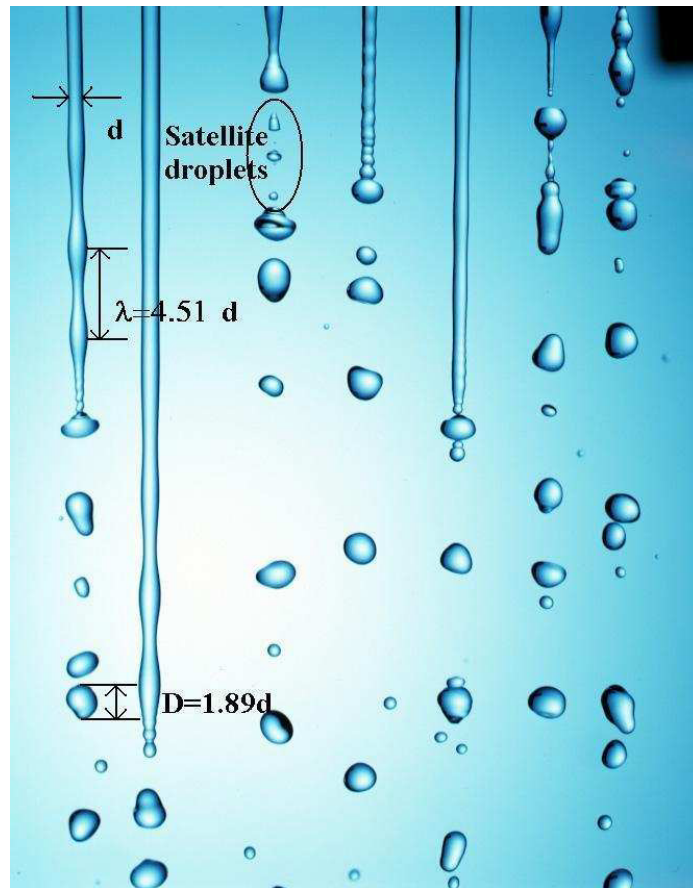


Fig. 1 Typical low-speed jet in the Rayleigh regime. Experimental image by Adam Hart-Davis [41]. (Reprinted by permission of Adam Hart-Davis.)

The coefficient of the w term accounts for viscous effects. McCarthy and Molloy [18] provided the maximum growth rate of Weber's Eq. (4):

$$w_m = \left(\sqrt{\frac{8\rho_l a^3}{\sigma}} + \frac{6\mu a}{\sigma} \right)^{-1} \quad (5)$$

The corresponding most dominant wavelength is

$$\lambda = \sqrt{2\pi d} \sqrt{1 + \frac{3\mu}{\sqrt{2\rho_l a \sigma}}} \quad (6)$$

Nonlinear simulations for viscous [19] and inviscid [13, 20] flows show comparable results for low-speed jets as well; the presence of viscosity only seems to decrease the rate at which the instability grows, not the shape of the wave.

4. STERLING-SLEICHER EQUATION

The greatest shortcoming of Rayleigh and Weber equations is due to the neglect of aerodynamic forces on the liquid jet. Sterling-Sleicher [7] (hereafter referred to as SS) had developed the dispersion equation that takes into account the aerodynamic effects; the general SS equation is

$$\begin{aligned} & \left[\frac{\xi I_0(\xi)}{2I_1(\xi)} + \epsilon \frac{\xi K_0(\xi)}{2K_1(\xi)} \right] w^2 \\ & + \left(2i\epsilon \frac{U\xi^2 K_0(\xi)}{2aK_1(\xi)} + \frac{\mu\xi^2}{\rho_l a^2} \left[2\xi \frac{I_0(\xi)}{I_1(\xi)} - 1 + \frac{2\xi^2}{\xi_1^2 - \xi^2} \left[\xi \frac{I_0(\xi)}{I_1(\xi)} - \xi_1 \frac{I_0(\xi_1)}{I_1(\xi_1)} \right] \right] \right) w \\ & = \frac{\sigma}{2\rho_l a^3} (1 - \xi^2)\xi^2 + \epsilon \frac{U^2 \xi^3}{2a^2} \frac{K_0(\xi)}{K_1(\xi)} \end{aligned} \quad (7)$$

where

$$\xi = ka \quad \xi_1^2 = \xi^2 + \frac{\omega a^2 \rho}{\mu} \quad \epsilon = \frac{\rho_g}{\rho_l} \quad (8)$$

In the absence of gas phase and viscosity (i.e., $\epsilon = \mu = 0$), the SS equation (7) reduces to Rayleigh's result. In addition, the general SS equation (7) can be written as follows:

$$\left[\frac{\xi I_0(\xi)}{2I_1(\xi)} + \epsilon \frac{\xi K_0(\xi)}{2K_1(\xi)} \right] w^2 + \left[i\epsilon \frac{U\xi^2 K_0(\xi)}{aK_1(\xi)} \right] w = \frac{\sigma}{2\rho_l a^3} (1 - \xi^2)\xi^2 + \epsilon \frac{U^2 \xi^2}{2a^2} \frac{K_0(\xi)}{K_1(\xi)} \quad (9)$$

Sterling-Sleicher considered the case where $\xi = ka < 1.0$, which implies that the wavenumber is small or the wavelength (i.e., $\lambda = 2\pi/k$) is large enough that it is of the order of the nozzle radius, a . In this case, the general SS equation is simplified substantially:

$$\omega^2 + \frac{3\mu\xi^2}{\rho_l a^2} \omega = \frac{\sigma}{2\rho_l a^3} (1 - \xi^2)\xi^2 + \epsilon \frac{U^2 \xi^3}{2a^2} \frac{K_0(\xi)}{K_1(\xi)} \quad (10)$$

It should be noted that a typographical error is present in the original Sterling-Sleicher article in the ϵ term. It should be U^2 , but it was set as just U . Here U is the "constant" and "uniform" jet speed. In the limit of $\xi \rightarrow \infty$ for an inviscid case, the SS equation (7) is essentially the same as the Kelvin-Helmholtz equation, which is used

to predict the smaller wavelengths (detailed proof of this claim is provided in the following section).

5. REITZ-BRACCO EQUATION

Further extension of the SS equation was presented by Reitz-Bracco [21] with the assumption that the liquid jet velocity is also a function of the radial direction [i.e., $U = U_g(r)$], as in the Orr-Sommerfeld equation [22, 23]. However, they later assumed $U = \text{constant}$. This equation of Reitz-Bracco (hereafter referred as RB) seems to be the most general dispersion expression available in the literature for the axisymmetric case.

$$\begin{aligned} & \omega^2 + 2vk^2 \left[\frac{I_1'(\xi)}{I_0(\xi)} - \frac{2kl}{k^2 + l^2} \frac{I_1(\xi)}{I_0(\xi)} \frac{I_1'(la)}{I_1(la)} \right] w \\ &= \frac{\sigma k}{\rho_l a^2} (1 - \xi^2) \left(\frac{l^2 - k^2}{l^2 + k^2} \right) \frac{I_1(\xi)}{I_0(\xi)} = \epsilon \left(U - \frac{i\omega}{k} \right)^2 k^2 \left(\frac{l^2 - k^2}{l^2 + k^2} \right) \frac{I_1(\xi)}{I_0(\xi)} \frac{K_0(\xi)}{K_1(\xi)} \end{aligned} \quad (11)$$

where

$$v = \frac{\mu}{\rho_l} \quad l^2 = k^2 + \frac{w}{v} \quad \lim_{v \rightarrow 0} \left(\frac{l^2 - k^2}{l^2 + k^2} \right) = 1.0 \quad (12)$$

It should be noted that Levich [6] had performed a similar analysis, the result of which is exactly the same as the RB equation except that Levich omitted the terms $\rho_g \omega^2$ and $\rho_g ikUw$ of the gas by assuming that the two terms are negligible compared to the terms $\rho_l \omega^2$ and $\rho_l ikUw$ of the liquid. In the absence of viscosity and the gas phase (i.e., $v = \epsilon = 0$), the RB equation (11) also recovers Rayleigh's result. Further, the RB equation (11) becomes the following if inviscid (i.e., $v = 0$):

$$\left[\frac{\xi}{2} + \epsilon \frac{\xi K_0(\xi)}{2K_1(\xi)} \right] w^2 + \left[i\epsilon \frac{U\xi^2 K_0(\xi)}{aK_1(\xi)} \right] w = \frac{\sigma}{2\rho_l a^3} (1 - \xi^2) \xi^2 + \epsilon \frac{U^2 \xi^3}{2a^3} \frac{K_0(\xi)}{K_1(\xi)} \quad (13)$$

This is exactly the same as the inviscid case of the SS equation (9) except for the coefficient of w^2 . This difference originated from Sterling-Sleicher's uniform jet speed (i.e., $U = \text{constant}$) assumption, which differs from Reitz-Bracco's jet velocity approximation with the gas velocity as a function of the radial direction. It is interesting to note that both the inviscid SS equation (9) and the RB equation (13) are reduced to the following expression in the limit as $\xi \rightarrow \infty$:

$$\omega^2 = \epsilon U^2 k^2 - \frac{\sigma k^3}{\rho_l} \quad (14)$$

where we have used the approximations $\lim_{\xi \rightarrow \infty} I_0(\xi)/I_1(\xi) = 0$, $\lim_{\xi \rightarrow \infty} K_0(\xi)/K_1(\xi) = 1$ (see Pearson [24]), and $\rho_l \gg \rho_g$. This Eq. (14) is essentially the Kelvin-Helmholtz equation [1, 25].

6. PONSTEIN'S EQUATION

In this section, the linear theory of Ponstein [5] is discussed. His work, published in 1959 in *Applied Scientific Research*, has not been well recognized in the atomization community. The work not only extended Rayleigh's [2, 26] analysis to include gas-phase effects, it also considered column rotation (swirl) in an analysis published long before Sterling-Sleicher (1975), and even before Levich (1962).

Ponstein considered two cases: a rotating liquid column in gas phase and a rotating bubble (or gas) column in a liquid surrounding for the second case. A uniform liquid column in vacuum was well known by Rayleigh [2], who predicted the most dominant wavelength, $\lambda = 4.51d$. Rayleigh [26] also considered a uniform bubble column in liquid whose solution is

$$\omega^2 = \frac{\sigma}{\rho_l a^3} (1 - k^2 a^2) \xi \frac{K_1(\xi)}{K_0(\xi)} \quad (15)$$

This equation predicts a most unstable wavelength, $\lambda = 6.48d$. For an axisymmetric rotating bubble column (based on $e^{i\omega t}$), Ponstein gives the following result:

$$\omega^2 = \left[\frac{\sigma}{\rho_l a^3} (1 - k^2 a^2) - \left(\frac{\Gamma}{2\pi a^2} \right)^2 \right] \xi \frac{K_1(\xi)}{K_0(\xi)} \quad (16)$$

where Γ is the circulation around the ring (or column), which can be estimated as $\Gamma = (2\pi a)V_\theta$ from Saffman [27]. Here V_θ is the tangential velocity of the ring surface. For a nonrotating case (i.e., $\Gamma = 0$), Eq. (16) recovers Rayleigh's result in Eq. (15). In this case, circulation has a stabilizing influence as indicated by the negative sign on the Γ term. The faster it rotates, the more stable the bubble ring is. Detailed discussion of Eq. (16) is available in Lundgren and Mansour [28], where they modeled the evolution of the bubble vortex-ring using the boundary integral method. An interesting example of the bubble vortex-ring of Dolphin is discussed by Shariff [29].

Ponstein gives the following result for the second case he considered, a rotating liquid column in gas:

$$\omega^2 = \left[\frac{\sigma}{\rho_l a^3} (1 - k^2 a^2) + (1 - \epsilon) \left(\frac{\Gamma}{2\pi a^2} \right)^2 \right] \xi \frac{I_1(\xi)}{I_0(\xi)} + \epsilon U^2 k^2 \frac{I_1(\xi)}{I_0(\xi)} \frac{K_0(\xi)}{K_1(\xi)} \quad (17)$$

If we consider nonrotating (i.e., $\Gamma = 0$) and nonaerodynamic effect (i.e., $U = \epsilon = 0$), Rayleigh's result is recovered. Here, circulation has a destabilizing effect as indicated by the positive sign on the Γ term. The faster the column rotates, the more unstable it becomes.

Increasing gas density ϵ serves to aid in stabilizing the column circulation term, but destabilizes the dominant aerodynamic (U^2) term.

Considering the nonrotating case with aerodynamic effect, Ponstein's equation (17) can be written as

$$\omega^2 = \frac{\sigma}{\rho_l a^3} (1 - k^2 a^2) \xi \frac{I_1(\xi)}{I_0(\xi)} + \epsilon U^2 k^2 \frac{I_1(\xi)}{I_0(\xi)} \frac{K_0(\xi)}{K_1(\xi)} \quad (18)$$

For $\xi < 1.0$, it is known that $I_1(\xi)/I_0(\xi) \approx (\xi)/2$. Applying this identity, Eq. (18) is rewritten as

$$\omega^2 = \frac{\sigma}{2\rho_l a^3} (1 - k^2 a^2) (\xi)^2 + \epsilon \frac{U^2 (\xi)^3}{2a^2} \frac{K_0(\xi)}{K_1(\xi)} \quad (19)$$

This result is exactly the same as the inviscid case of the dispersion relation derived by Sterling-Sleicher in Eq. (10).

7. TAYLOR'S EQUATION

Taylor [4] derived the following relation based on his aerodynamic theory:

$$\frac{w}{kU} = \sqrt{\frac{\rho_g}{\rho_l}} 2xg(x) \quad (20)$$

where x is the nondimensional wavelength of Reitz and Bracco [21] and $g = g(x, T)$ is the function of the Taylor number, T .

$$x = \frac{\rho_g U^2}{\sigma k} \quad T = \frac{\rho_l}{\rho_g} \left(\frac{\sigma}{\mu U} \right)^2 = \frac{\rho_l}{\rho_g} \left(\frac{\text{Re}}{\text{We}_{l,d}} \right)^2 \quad (21)$$

with $\text{Re} = \rho_l U d / \mu$ and $\text{We}_{l,d} = \rho_l U^2 d / \sigma$. The RB equation (11) in the limit of $\xi \rightarrow \infty$ with viscosity (i.e., $\nu \neq 0$) is as follows:

$$(w + 2\nu k^2)^2 + \frac{\sigma k^3}{\rho_l} - 4\nu^2 k^3 \sqrt{k^2 + \frac{w}{\nu}} + \frac{\rho_g}{\rho_l} (w + iUk)^2 = 0 \quad (22)$$

Expanding Eq. (22) yields:

$$\left(1 + \frac{\rho_g}{\rho_l} \right) \left(\frac{w}{Uk} \right)^2 = \frac{\rho_g}{\rho_l} - \frac{\sigma k}{\rho_l U^2} - i \frac{\rho_g}{\rho_l} \frac{2w}{Uk} + \frac{1}{U^2 k^2} \left(4\nu^2 k^3 \sqrt{k^2 + \frac{w}{\nu}} - 4\nu k^2 w - 4\nu^2 k^4 \right) \quad (23)$$

This equation (23) is modified in the form of Taylor's equation (20) assuming that (ρ_g/ρ_l) (w/Uk^2) is negligible compared to $(w/Uk)^2$ and the temporal growth rate of the ρ_g/ρ_l term in the imaginary part of w is also negligible (which is similar to what Levich had assumed in his analysis [6]),

$$\frac{w}{Uk} = \sqrt{\frac{\rho_g}{\rho_l} h(x)} \quad (24)$$

where

$$h(x) = \sqrt{1 - \frac{1}{x} + \frac{\rho_l \chi}{U^2 k^2 \rho_g}} \quad \chi = 2 \left(2v^2 k^3 \sqrt{k^2 + \frac{w}{v}} - 2v \quad k^2 w - 2v^2 k^4 \right) \quad (25)$$

If we hypothesize that the RB equation (24) is the same as Taylor's equation (20), the following relation can be set:

$$2x g(x) = h(x) \quad (26)$$

Reitz and Bracco [21] also defined a function $f(x) = x g(x)$. The numerical solution of Eq. (24) was given by Reitz and Bracco. The most dominant nondimensional wavelength x_m was found to be 1.5 and thus $f(x_m) = \sqrt{3}/6 \approx 0.2887$ as $T_a \geq 1.0$ (see Bracco [30]). Though the value of $f(x_m) = \sqrt{3}/6$ was first found by G. I. Taylor [4]) (and was mentioned in Ranz's article [31]), it seems that the most dominant nondimensional wavelength $x_m = 1.5$ [which gives $f(x_m) = \sqrt{3}/6$] was noted by Reitz and Bracco [21]. The same results have been found using the KH equation (14), which is significantly simpler than Eq. (24). The KH equation (14) can be written in the form of Taylor's equation (20):

$$\frac{w}{kU} = \sqrt{\frac{\rho_g}{\rho_l} \left(1 - \frac{1}{x} \right)^{1/2}} \quad (27)$$

Note that the KH equation (14) is valid under inviscid (i.e., $v = 0$) assumption. If this is the same as Taylor's equation (20), then $2xg(x) = [1 - (1/x)]^{1/2}$ can be set:

$$g(x) = \frac{1}{2x} \left(1 - \frac{1}{x} \right)^{1/2} \quad (28)$$

The $f(x)$ and $g(x)$ as functions of the nondimensional wavelength x are plotted in Fig. 2. The $g(x_m)$ can be found by taking the derivative of Eq. (28) with respect to x .

$$\frac{dg(x)}{dx} = \frac{1 - 2xy}{4x^3 y^{1/2}} \quad (29)$$

where $y = 1 - 1/x$. Let $1 - 2xy = 0$ to find the most dominant nondimensional wavenumber, x_m . This gives the following analytical results:

$$x_m = 1.5 \quad f(x_m) = x_m g(x_m) = \frac{\sqrt{3}}{6} \tag{30}$$

This shows that the viscosity is of little importance since no difference is seen in x_m and $f(x_m)$ values between Reitz and Bracco's numerical result and our analytical results using the KH equation (14) (see Fig. 2).

Wu et al [8] assumed that the initial droplet diameter, D , might be proportional to the length of the most unstable wavelength, λ :

$$D = B\lambda \tag{31}$$

where

$$\lambda = \frac{2\pi}{k_m} = \frac{2\pi}{(U^2 \rho_g) / (\sigma x_m)} = \frac{2\pi \sigma}{U^2 \rho_g} x_m = \frac{2\pi \sigma}{U^2 \rho_g} (1.5) = \frac{3\pi \sigma}{U^2 \rho_g} \tag{32}$$

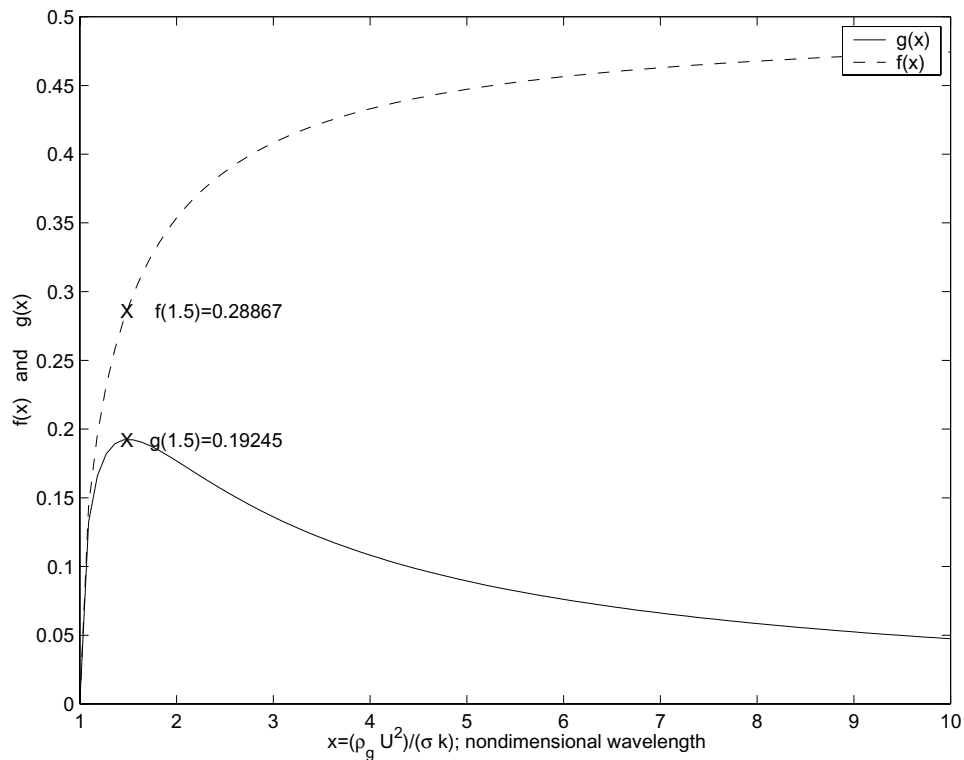


Fig. 2 The functions $g(x)$ by Taylor [4] and $f(x) = xg(x)$ by Reitz and Bracco [21] as functions of nondimensional wavenumber $x = (\rho_g U^2) / (\sigma k)$.

B is a constant that is empirically approximated. Wu, Reitz, and Bracco [8] gave $B \approx 4.5$, based on the curve-fit of their experimental data. Applying this Eq. (32) to Hoyt and Taylor's case [11], which is discussed in detail in the next section (i.e., $\sigma_{\text{H}_2\text{O}} = 0.0734 \text{ kg/s}^2$, $\rho_{\text{air}} = 1.23 \text{ kg/m}^3$, $U = 21 \text{ m/s}$, and $d = 6.35 \text{ mm}$, thus $We_g = 46.9$), the most unstable wavelength is $\lambda \approx d/5$. The wavelength overpredicts the value observed in Hoyt and Taylor's experiment (i.e., $\lambda \approx d/13.8$). It should be noted that Eq. (32) is capable of producing very small wavelengths with large U and ρ_g , which is the case of Wu et al. [8]; this aerodynamic theory works well for their atomizing jets of the shear layer-driven instability.

8. BOUNDARY-LAYER INSTABILITY ANALYSIS

Here we should note that the classical column-based theories we have presented are all classified as temporal stability analyses. While these tend to be the most useful in implementation in atomization models, there are also spatial and spatiotemporal theories addressing other mechanisms of instability growth. For low-speed jets in the Rayleigh regime, the temporal-based theory has been shown to be appropriate in both linear and nonlinear regimes; but at higher jet speeds there is less evidence as to the preferred approach. A more recent work by Lin and Chen [32] addresses this issue in more detail.

None of the conventional linear stability theories can account for the largely axisymmetric waves observed by Hoyt and Taylor [11] in their famous 1977 experiments. In this experiment, a carefully machined nozzle was used to provide a favorable pressure gradient to a reasonably high-speed jet such that turbulence effects were minimized. The resultant waves formed on the surface of the water jet showed wavelengths $\lambda \approx d/13.8$, which is not predicted well by the linear theories discussed above. These researchers theorized that the thickness of the boundary layer at the orifice exit plane could play a significant role in explaining the observed wavelength. It was suspected that the point of inflection due to change in velocity profile from a no-slip to a free-surface edge condition was responsible for the instability and the subsequent wave growth. Shkadov [33] was another researcher working on this theory at the time.

For this reason, we review the classical boundary-layer instability based on the Orr-Sommerfeld equation. Using (1) the solution by Betchov and Criminale [34] for the fully developed 2-D steady parallel laminar flow, (2) the perturbation method [22], and (3) linearization, the 2-D Navier-Stokes equations can be written as follows:

$$(u - c) \left(\hat{v} - \frac{1}{\alpha^2} \hat{v}'' \right) + \frac{1}{\alpha^2} \hat{v} u'' = \frac{1}{\text{Re}_{\delta_2} i \alpha} \left(2 \hat{v}'' - \alpha^2 \hat{v} - \frac{1}{\alpha} \hat{v}''' \right) \quad (33)$$

where $u = u(y)$ is the axial velocity profile in the y direction, $c = c_r + ic_i$ is the complex phase velocity, α is the wavenumber, $\hat{v} = \hat{v}(y)$ is the amplitude of the radial perturbation in the y direction, and $\text{Re}_{\delta_2} = U \delta_2 / \nu$. This is called the Orr-Sommerfeld equation. Sometimes different notations [i.e., $\hat{v}(y) = -i \alpha \phi(y)$] are used by researchers (see Panton [23] and/or Schlichting [22]). It should also be noted that $\phi(y)$ is not velocity potential, but complex amplitude function for the streamfunction. There is no analytic solution to Eq. (33), but the numerical solution for a wide range of values of frequency and Re_{δ_2} is available by Jordinson [34].

Considering the inviscid case of the Orr-Sommerfeld equation (33) (i.e., $\text{Re}_{\delta_2} \rightarrow \infty$), the following equation is obtained:

$$(u - c) \left(\hat{v} - \frac{1}{\alpha^2} \hat{v}'' \right) + \frac{1}{\alpha^2} \hat{v} u'' = 0 \quad (34)$$

This is called the Rayleigh equation. Lord Rayleigh (1880–1913) provided a theorem based on his equation (34), that “Velocity profiles with points of inflection are unstable.” Rayleigh proved that the presence of a *point of inflection* is a *necessary* (though it is not *sufficient*) condition for the appearance of unstable waves. This is a powerful statement, as it can be used to classify the flow regime: laminar to turbulent flows. For example, the velocity profile contains no point of inflection under favorable pressure gradient (i.e., $\partial P/\partial x < 0$). Generally, it is fair to state that the flow is laminar in such a case. On the other hand, a point of inflection can be found in an adverse pressure gradient (i.e., $\partial P/\partial x > 0$), where the flow is sometimes unstable and eventually this may lead to turbulent flow.

The influence of gas density, and hence aerodynamic forces on the interface, has been widely investigated experimentally. Reitz and Bracco [21] observed a substantial difference in the atomization mechanism when the liquid jet was injected in different gases (i.e., $\rho_{N_2} = 6 \text{ kg/m}^3$ and $\rho_{Xe} = 23 \text{ kg/m}^3$). Wu et al. [36] have reported a change in droplet size for primary atomization when a different gas density was tested for the same liquid jet. From this basis one may conclude that the aerodynamic interaction at the surface of the jet does alter wave growth—i.e., that aerodynamic forces are of sufficient magnitude to contribute to the instability.

Shkadov’s theory [33] states that the velocity profile of a liquid is independent of gas density, which seems contradictory to the experimentally observed trend. This dilemma is probably due to the high gas–liquid density ratio, which causes the growth rate due to the aerodynamic term to dominate as compared to the growth rate due to the vortices rollup (at the point of inflection of the velocity profile during the relaxation process), thereby invalidating Shkadov’s theory. In addition, the droplet sizes are strongly dependent on secondary atomization at high jet speed and high gas density conditions.

Clearly, the influence of the gas is regime-dependent, but the fundamental instability mechanism is present in all regimes. The fundamental questions which should be asked are: “Will instability occur in the absence of gas phase? If so, where is that instability mechanism originating from?”

Hoyt and Taylor [10] did not observe differences in wave structure with differing external air flows in their experiments. The axisymmetrically disturbed short wavelength observed near the nozzle exit is present regardless of magnitude or direction of the air velocity. Hoyt and Taylor concluded that this phenomenon has “no discernible effect of relative air velocity.” In spite of Hoyt and Taylor’s effort in this regard, their result has not well been recognized in the atomization community. For many years, the notion that vorticity at the nozzle exit is responsible for the atomization has been overshadowed by the aerodynamic linear theory and the experiment which showed a significant difference in spray structure with the change in gas density.

Shkadov [32] provides the solution of the Rayleigh’s Eq. (34) and proves that the amplitude of surface waves grows in the downstream direction, as the jet velocity profile relaxes. This eigenvalue problem has also been solved by Brennen [9]. Brennen provided

the boundary-layer instability analysis. He considered separated boundary-layer flow over the planar plate using a Gaussian velocity profile. This resulted in

$$\gamma = 2\pi f \frac{\delta_2}{U} \quad (35)$$

where γ is the nondimensional frequency, f is the dimensional frequency [Hz], δ_2 is the momentum thickness [m], and U is the speed of the uniform flow [m/s]. Brennan concluded that $\gamma = 0.175$ was the nondimensional frequency which would give maximum amplification at the flow separation point.

Applying $\gamma = 0.175$ to the Hoyt and Taylor case [11],

$$f = \frac{\gamma U}{2\pi \delta_2} = \left(\frac{0.175}{2\pi} \right) \left(\frac{21 \text{ m/s}}{1.2 \times 10^{-5} \text{ m}} \right) = 48,741 \text{ Hz} \quad (36)$$

Note that the boundary-layer momentum thickness, δ_2 , can be approximated using Blasius' solution [37] for laminar flow assuming that $\delta_2 \ll a$:

$$\frac{\delta_1}{x} = \frac{1.721}{\sqrt{\text{Re}_x}} \quad \frac{\delta_2}{x} = \frac{0.664}{\sqrt{\text{Re}_x}} \quad (37)$$

where $\text{Re}_x = Ux/\nu$ and δ_1 is the displacement thickness. Assuming that the wave speed is about the same as that of the liquid jet U ,

$$\lambda \approx \frac{U}{f} = \frac{21 \text{ m/s}}{48,741 \text{ Hz}} = 0.43 \text{ mm} = \frac{d}{14.8} \quad (38)$$

While this was a theoretically predicted value, Hoyt and Taylor's experimental observation of the axisymmetrically disturbed wavelength was about $\lambda \approx 0.46 \text{ mm} = d/13.8$, as shown in Fig. 3 (note: $d = 6.35 \text{ mm}$). The comparison between theory and experiment was excellent.

McCarthy and Molloy's experiment [18] provides further confirmation of the role of the momentum thickness in wave formation at the orifice exit plane. They varied the nozzle-to-diameter ratio (i.e., l/d) and observed the effect of l/d on "laminar" jet structure. In their article [18], it was not mentioned that the jets had distinctive axisymmetric waves for different orifice designs, yet the experimental images do contain these structures as shown in Fig. 4, reproduced from their article. Farther downstream, the jets become turbulent (see cases $l/d = 5$ and 10 in Fig. 5) and result in the primary atomization.

To compare the McCarthy and Molloy results with Brennan's theory, we assume that boundary-layer development inside the passage can be approximated by boundary-layer growth on a flat plate. Clearly, this assumption becomes poor when the boundary layer is a substantial fraction of the orifice radius, but one could use a numerical analysis or more elaborate theory to ascertain momentum thicknesses at the orifice exit plane more accurately. The errors result from free-stream pressure gradients which develop as the boundary layer builds in the passage. A thorough review of turbulent momentum thickness is given

by Klein [38]. Given this caveat, the predicted δ_2 values using this technique, when implemented in Brennen's equation, show good agreement with the observed wavelengths from the McCarthy and Molloy experiments as presented in Table 1. One can also note from Table 1 that the δ_2 values are all quite small relative to the orifice radius, thereby lending credence to the simple approach of assuming flat-plate boundary-layer growth.

9. COMPARISON OF THE LINEAR MODELS

It is useful to compare the wavelengths predicted by the liquid column theories and the boundary-layer theory for the same atomizer. In Fig. 6, wavelength predicted by Brennen's theory is plotted as a function of jet speed for various l/d and is compared with the SS and KH liquid column-based analyses.

The results obtained by the Sterling-Sleicher equation (10) and that obtained by the Kelvin-Helmholtz equation (14) are essentially the same at the higher jet speeds, indicating that the KH mechanism is dominant for atomizing jets. The Reitz and Bracco equation (13) (though not plotted in Fig. 6) gives results very similar to the Sterling and Sleicher result, as noted in prior discussion. These column-based results show a strong dependence on jet velocity at the lower speeds, with asymptotic behavior at the high jet speeds. The boundary-layer-based results are also provided in Fig. 6 for various orifice lengths. These results show a more modest variation in critical wavelength at the lower injection velocities, with similar asymptotic behavior at the high jet speeds. Results from the boundary-layer-based analysis show a strong influence of orifice l/d , while the column-based analysis does not include this parameter. In general, the boundary-layer-based results predict smaller wavelengths at the low jet speeds and larger wavelengths at the higher jet speeds when compared to the column-based results.

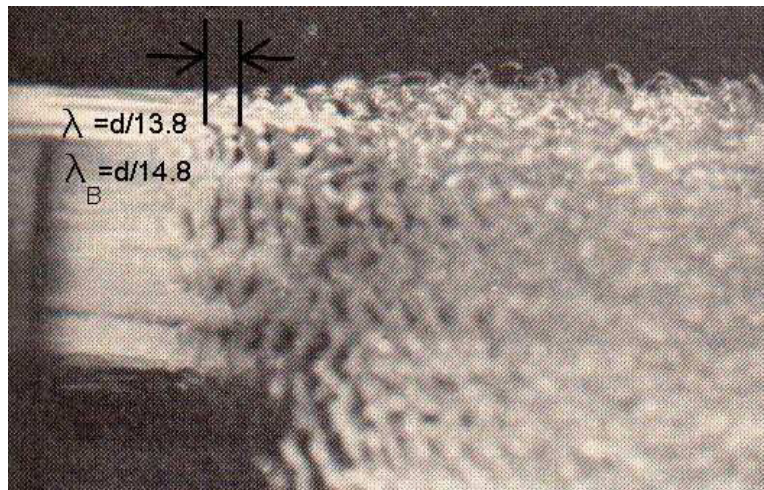


Fig. 3 Typical water jet into air in the atomization regime. Experimental image by Hoyt and Taylor [10], which shows the most dominant wavelength $\lambda = d/13.8$ while Brennen's theory predicts $\lambda_B = d/14.8$. (Reprinted by permission of the *Journal of Fluid Mechanics*.)

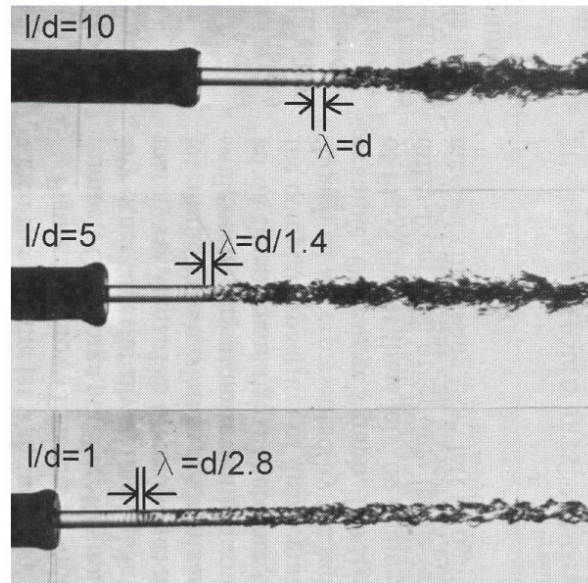


Fig. 4 McCarthy and Molloy's experiment [18] for $l/d = 10, 5,$ and 1 : The most dominant wavelength appears subsequent to the laminar region which can be scaled by Brennen's [9] theory. (Reprinted by permission of Elsevier Science.)

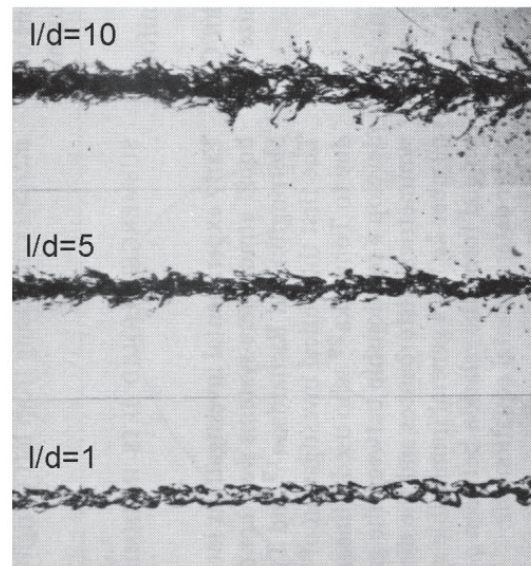


Fig. 5 McCarthy and Molloy's experiment [18] for $l/d = 10, 5,$ and 1 in the farther downstream. Droplet size is not scaled by the most dominant wavelength. (Reprinted by permission of Elsevier Science.)

Table 1 Summary for McCarthy and Molloy's Experiment [18]

l/d^a	Re_x^b	δ_1/d	δ_2/d	Re_{δ_2}	f^c [Hz]	λ^d	λ_{exp}
1	4,748	1/40.04	1/103.8	46	22,758	$d/2.89$	$d/2.8$
5	23,738	1/17.90	1/46.41	102	10,178	$d/1.3$	$d/1.4$
10	47,477	1/12.66	1/32.82	145	7,197	$1.1d$	$1.0d$

^a l/d = nozzle length-to-diameter ratio.
^b $Re_x = Ul/\nu$.
^{c,d} Brennen's Eqs. (36) and (38), respectively.
 Note: Blasius' solution is used for δ_1 and δ_2 estimation.

Unfortunately, the influence of turbulence, especially at the higher jet speeds, makes it difficult to perform experiments to compare the two theories. The axisymmetrically perturbed waves are not observable when the jet flow is already turbulent flow at the nozzle exit (see Fig. 1 of Wu et al. [39]). However, the flow at the Hoyt and Taylor nozzle exit is nearly laminar flow, as the flow is laminarized through highly contracted nozzle geometry

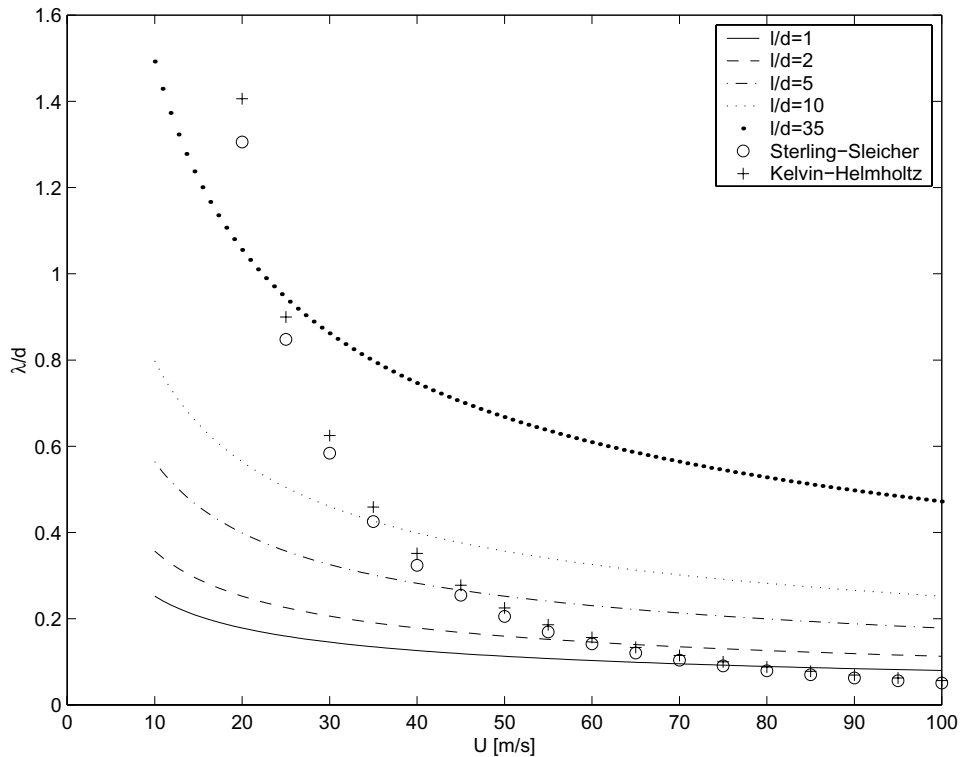


Fig. 6 Variation of the theoretically predicted boundary-layer waves as well as that of the Sterling-Sleicher equation (10) and the Kelvin-Helmholtz equation (14) as a function of jet speed for various l/d . A water jet into air is considered: $\nu = 1.12 \times 10^{-6} \text{ m}^2/\text{s}$ and $d = 1 \text{ mm}$. Second wind-induced regime for $26.76 \text{ m/s} < U < 48.86 \text{ m/s}$ and atomization regime for $U > 48.86 \text{ m/s}$.

under the favorable pressure gradient [11]. Their carefully conducted experiment, which substantially reduced all other possible perturbation sources (i.e., such as turbulence and cavitation), made observation of the boundary-layer waves possible. For their water jet (laminar at the nozzle exit), the Reynolds number based on the momentum thickness (Re_{δ_2}) is about 225, while the Blasius solution indicates that the flow should be turbulent for $Re_{\delta_2} > 200$.

This problem probably occurs because the favorable pressure gradient has shifted the shape factor (i.e., $H = \delta_1/\delta_2$) the critical Reynolds number ($Re_{\delta_2, \text{crit}}$) has increased. It should be noted that a slight decrease in H can result in a substantial increase in $Re_{\delta_2, \text{crit}}$ [37, 40]. At this stage of research, it is not clear where the $Re_{\delta_2, \text{crit}}$ lies for the liquid jet. In Fig. 7, we have considered a laminar water jet into air. It is shown that Re_{δ_2} increases with increasing l/d . In reality, it is not guaranteed that the flow at the nozzle exit is laminar for high l/d . However, one will have a better chance of observing the boundary-layer waves if $Re_{\delta_2} < Re_{\delta_2, \text{crit}}$. It certainly would be interesting to generate additional experimental data for these conditions.

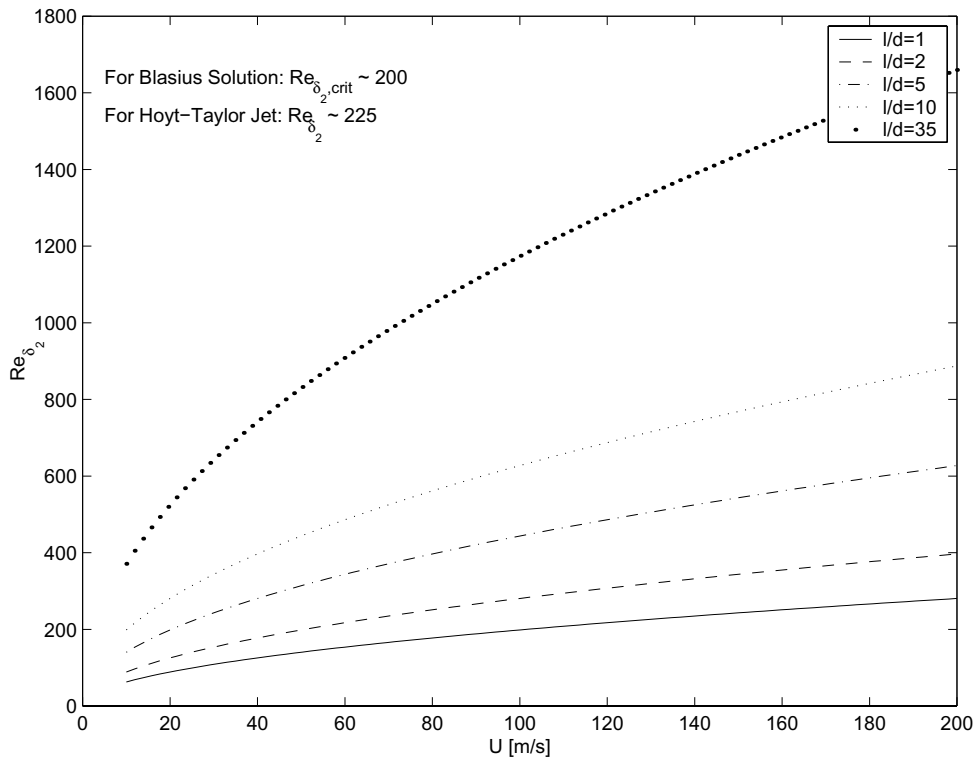


Fig. 7 Variation of the theoretically predicted Reynolds number based on the momentum thickness as a function of jet speed for various l/d : the same case as in Fig. 6.

10. CONCLUSIONS

Linear analyses based on liquid column- and boundary-layer-based methodologies have been compared and contrasted. The boundary-layer-based analysis has the advantage that it addresses the orifice geometry as a primary influence in determining the most unstable wavelength. The column-based theories have been shown to be largely equivalent in the atomization regime, due to the dominance of the Kelvin-Helmholtz instability mechanism at these conditions. In performing a sample comparison of the two methods for a water jet, the boundary-layer-based scheme tends to predict smaller critical wavelengths at low-speed conditions and larger critical wavelengths at high injection speeds. While the column-based analysis has received more attention in the community, the boundary-layer-based approach has been shown to have merit based on limited experiments aimed at addressing this mechanism.

REFERENCES

1. P. G. Drazin and W. H. Reid, *Hydrodynamic Stability*, pp. 14–28, Cambridge University Press, New York, NY, 1981.
2. W. S. Rayleigh, On the Instability of Jets, *Proc. Lond. Math. Soc.*, vol. 10, no. 4, 1878.
3. C. Weber, Zum Zerfall eines Flüssigkeitsstrahles. *Z. Angew. Math. Mech.*, vol. 11, pp. 138–245, 1931.
4. G. K. Batchelor (ed.), *Collected Works of G. I. Taylor*, Cambridge University Press, Cambridge, MA, 1958.
5. J. Ponstein, Instability of Rotating Cylindrical Jets, *Appl. Sci. Res.*, vol. 8, no. 6, pp. 425–456, 1959.
6. V. G. Levich, *Physicochemical Hydrodynamics*, pp. 639–646, Prentice Hall, Englewood Cliffs, NJ, 1962.
7. A. M. Sterling and C. A. Sleicher, The Instability of Capillary Jets, *J. Fluid Mech.*, vol. 68, no. 3, pp. 477–495, 1975.
8. K. J. Wu, R. D. Reitz, and F. V. Bracco, Measurements of Drop Size at the Spray Edge near the Nozzle in Atomizing Liquid Jets, *Phys Fluids*, vol. 29, no. 4, pp. 941–951, 1986.
9. C. Brennen, Cavity Surface Wave Patterns and General Appearance, *J. Fluid Mech.*, vol. 44, no. 1, pp. 33–49, 1970.
10. J. W. Hoyt and J. J. Taylor, Waves on Water Jets, *J. Fluid Mech.*, vol. 83, pp. 119–127, 1977.
11. J. W. Hoyt and J. J. Taylor, Turbulence Structure in a Water Jet Discharging in the Air, *Phys. Fluids*, vol. 20, no. 10, pp. s253–s257, 1977.
12. J. W. Hoyt and J. J. Taylor, Effect of Nozzle Boundary Layer on Water Jets Discharging in the Air, in *Jets and Cavities—Int. Symp.*, pp. 93–100, ASME, Miami Beach, FL, Nov. 17–22, 1985.
13. N. N. Mansour and T. T. Lundgren, Satellite Formation in Capillary Jet Breakup, *Phys. Fluids*, vol. 2, pp. 1141–1144, 1990.
14. P. Lafrance, Nonlinear Breakup of a Laminar Liquid Jet, *Phys. Fluids*, vol. 18, p. 428, 1975.
15. D. F. Rutland and G. J. Jameson, Theoretical Prediction of the Sizes of Drops Formed in the Breakup of Capillary Jets, *Chem. Eng. Sci.*, vol. 25, pp. 1689–1698, 1970.
16. C. A. Spangler, J. H. Hilbing, and S. D. Heister, Nonlinear Modeling of Jet Atomization in the Wind-Induced Regime, *Phys. Fluids*, vol. 7, p. 964, 1995.
17. D. F. Rutland and G. J. Jameson, A Non-linear Effect in the Capillary Instability of Liquid Jets, *J. Fluid Mech.*, vol. 46, no. 2, pp. 267–271, 1971.

18. M. J. McCarthy and N. A. Molloy, Review of Stability of Liquid Jets and the Influence of Nozzle Design, *Chem. Eng. J.*, vol. 7, pp. 1–20, 1974.
19. D. W. DePaoli, T. C. Scott, and O. A. Basaran, Oscillation Frequencies of Droplets Held Pendant on a Nozzle, *Sep. Sci. Technol.*, vol. 27, no. 15, pp. 2071–2082, 1992.
20. C. A. Spangler, J. H. Hilbing, and S. D. Heister, Nonlinear Modeling of Jet Atomization in the Wind-Induced Regime, *Phys. Fluids*, vol. 7, no. 5, pp. 964–971, 1995.
21. R. D. Reitz and F. V. Bracco, Mechanism of Atomization of a Liquid Jet, *Phys. Fluids*, vol. 25, no. 10, pp. 1730–1742, 1982.
22. H. Schlichting, *Boundary Layer Theory*, pp. 461–463, McGraw-Hill, New York, NY, 1979.
23. R. L. Panton, *Incompressible Flow*, 2d ed., pp. 460–470, 718–727, 739–741, Wiley, New York, NY, 1996.
24. C. E. Pearson, *Handbook of Applied Mathematics*, pp. 349–350, 361, Van Nostrand Reinhold, New York, NY, 1974.
25. G. K. Batchelor, *An Introduction to Fluid Dynamics*, pp. 511–517, 521–526, Cambridge University Press, New York, NY, 1999.
26. W. S. Rayleigh, On the Instability of Cylindrical Fluid Surfaces, *Phil. Mag.*, vol. 34, no. 207, 1892.
27. P. G. Saffman, The Number of Waves on Unstable Vortex Rings, *J. Fluid Mech.*, vol. 84, no. 4, pp. 625–639, 1978.
28. T. T. Lundgren and N. N. Mansour, Vortex Ring Bubbles, *J. Fluid Mech.*, vol. 224, pp. 177–196, 1991.
29. K. Marten, K. Shariff, S. Psarakos, and D. J. White, Ring Bubbles of Dolphins, *Sci. Am.*, pp. 82–87, August 1996.
30. F. V. Bracco, Modeling of Engine Sprays, *SAE Trans., Fuels and Lubricants*, vol. 94, no. 850394, pp. 144–167, 1985.
31. W. E. Ranz, Some Experiments on Orifice Sprays, *Can. J. Chem. Eng.*, vol. 36, p. 175, 1958.
32. S. P. Lin and J. N. Chen, Role Played by the Interfacial Shear in the Instability Mechanism of a Viscous Gas in a Pipe, *J. Fluid Mech.*, vol. 376, pp. 37–51, 1998.
33. V. Y. Shkadov, Wave Formation on Surface of Viscous Liquid due to Tangential Stress, *Fluid Dynam.*, vol. 5, pp. 473–476, 1970.
34. R. Betchov and W. O. Criminale, *Stability of Parallel Flows*, 2d ed., p. 235, Academic Press, New York, NY, 1967.
35. R. Jordinson, The Flat Plate Boundary Layer. Part 1. Numerical Integration of the Orr-Sommerfeld Equation, *J. Fluid Mech.*, vol. 43, pp. 801–811, 1970.
36. P. K. Wu and G. M. Faeth, Aerodynamic Effects on Primary Breakup of Turbulent Liquids, *Atomization and Sprays*, vol. 3, pp. 265–289, 1993.
37. F. M. White, *Viscous Fluid Flow*, 2d ed., pp. 235, 269, 358, McGraw-Hill, New York, NY, 1991.
38. A. Klein, Review: Turbulent Developing Pipe Flow, *J. Fluids Eng.*, vol. 103, pp. 243–249, 1981.
39. P. K. Wu, L. K. Tseng, and G. M. Faeth, Primary Breakup in Gas/Liquid Mixing Layers for Turbulent Liquids, *Atomization and Sprays*, vol. 2, pp. 295–317, 1992.
40. A. R. Wazzan, C. Gazley, Jr., and A. M. O. Smith, Tollmien-Schlichting Waves and Transition, *Prog. Aerospace Sci.*, vol. 18, no. 2, pp. 351–392, 1979.
41. A. Hart-Davis, <http://www.freeimages.co.uk/>, in *Jet Flow in Rayleigh Regime*, 2001, <http://www.hd.org/Damon/photos/>.